

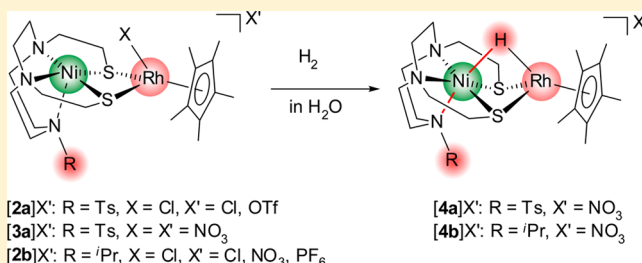
Hydride-Bridged NiRh Complexes with Tunable N₃S₂ Dithiolato Ligands and Their Utilization as Catalysts for Hydrogenation of Aldehydes and CO₂ in Aqueous Media

Bunsho Kure,* Ayami Taniguchi, Takayuki Nakajima, and Tomoaki Tanase*

Department of Chemistry, Faculty of Science, Nara Women's University, Kitauoya-nishi-machi, Nara, 630-8506, Japan

S Supporting Information

ABSTRACT: New N₃S₂ dithiolato ligands, 1,4-bis(2-mercaptoethyl)-7-R-1,4,7-triazacyclononane (RTACN-S₂H₂; R = Ts, ⁱPr) were synthesized and reacted with Ni^{II} ion to give mononuclear complexes [Ni(RTACN-S₂)] (R = Ts (**1a**), ⁱPr (**1b**)). Complexes **1a** and **1b** were further transformed by treatment with Rh^{III} species into a series of Ni^{II}Rh^{III} heterodimetallic compounds, [Ni(RTACN-S₂)RhCp^{*}X]X' (R = Ts, X = Cl, X' = Cl, OTf ([**2a**]X'); R = Ts, X = X' = NO₃ ([**3a**]NO₃); R = ⁱPr, X = Cl, X' = Cl, NO₃, PF₆ ([**2b**]X')). Complexes [**3a**]NO₃ and [**2b**]NO₃ were readily reacted with H₂ (0.1 MPa) in water at room temperature to afford hydride-bridged Ni^{II}Rh^{III} dinuclear complexes, [(RTACN-S₂)Ni(μ-H)RhCp^{*}]NO₃ (R = Ts ([**4a**]NO₃), ⁱPr ([**4b**]NO₃)), which were successfully characterized by X-ray crystallography. Upon the heterolytic activation of H₂, the Ni–Rh interatomic distances were dramatically decreased from 3.2130(6)–3.262(2) Å ([**2a**]OTf, [**2b**]NO₃, [**3a**]NO₃) to 2.6921(6)–2.7228(4) Å ([**4a**]NO₃, [**4b**]NO₃), resulting in semibridging Ni(μ-H)Rh cores. In addition, the stability of the hydride of [**4a**]⁺ and [**4b**]⁺ were interestingly tuned by varying the R group of the TACN ligand through *trans* influence at the Ni^{II} center (Ni–NR = 2.188(3) Å ([**4a**]⁺), 2.056(2) Å ([**4b**]⁺). In fact, [**4a**]⁺ was quite stable and capable of reducing benzaldehyde in water, although [**4b**]⁺ quickly decomposed under similar conditions. Catalytic hydrogenation of aldehydes and CO₂ in water has been established by using [**3a**]NO₃ and [**2a**]Cl as precursors of an active species, [**4a**]⁺, and found to be interestingly contrasted to the inactive precursor [**2b**]NO₃ with R = ⁱPr. These results indicated that the properties and reactivity of the Ni(μ-H)Rh complexes can be controlled by changing the substituents of the N₃S₂ supporting ligands.



INTRODUCTION

Development of new water-soluble organometallic catalysts has attracted rapidly growing attention because water is a naturally abundant and green (nontoxic, nonflammable, and non-hazardous) solvent, having its use to allow simple purification of organic products and pH-dependent selectivity.¹ In this regard, catalytic hydrogenations and hydrogen-transfer reactions of unsaturated compounds in water are highly desired industrial processes rather than establishing the applied principle of reduction by using stoichiometric hazardous hydride reagents, such as NaBH₄.² To date, several transition-metal complexes have been known to catalyze such reactions in water or aqueous biphasic media.³ However, active transition-metal hydride complexes have rarely been isolated and fully characterized because, in its general sense, these were very unstable in water.^{4,5} For example, Steckhan, Fish, Süß-Fink, and their co-workers independently reported water-soluble transfer hydrogenation catalysts that were converted *in situ* to the active hydride species, such as [RhCp^{*}(H)(bpy)]⁺ (Chart 1a, Cp^{*} = η⁵-pentamethylcyclopentadienyl, bpy = 2,2'-bipyridine) and [RhCp^{*}(H)(phen)]⁺ (phen = 1,10-phenanthroline),⁶ although their definitive structures have not been

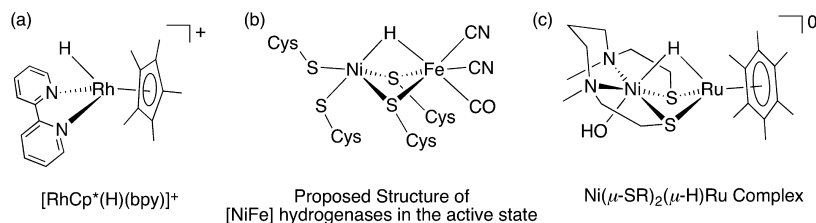
characterized, and thus, their detailed roles in the catalytic cycles were mostly hypothesized.

In nature, [NiFe] hydrogenases catalyze heterolytic activation of H₂ into a proton and hydride along with the reduction of substrates, such as methylene blue and NAD⁺, under ambient conditions in water.^{7,8} The active sites of [NiFe] hydrogenases in the Ni–C and Ni–R active states are believed to be consisting of Ni and Fe dimetal centers bridged by two thiolato and one hydride ligand (Chart 1b).⁸ Although many structural and functional models for [NiFe] hydrogenases have been prepared,⁹ only one substantial example has been reported by Kure and Ogo et al. on hydrogenation of small molecules catalyzed by a bithiolate-bridged dinuclear complex under ambient conditions in water,^{3g} wherein hydrogenation of aldehydes was catalyzed by the dinuclear NiRu complex in water, and the active hydride complex [Ni(OH)(μ-SR)₂(μ-H)Ru(η⁶-C₆Me₆)] ((HSR)₂ = N,N'-dimethyl-N,N'-bis(2-mercaptoethyl)-1,3-propanediamine, Chart 1c) was isolated to reveal that the hydroxo group on the Ni center *trans* to the μ-H

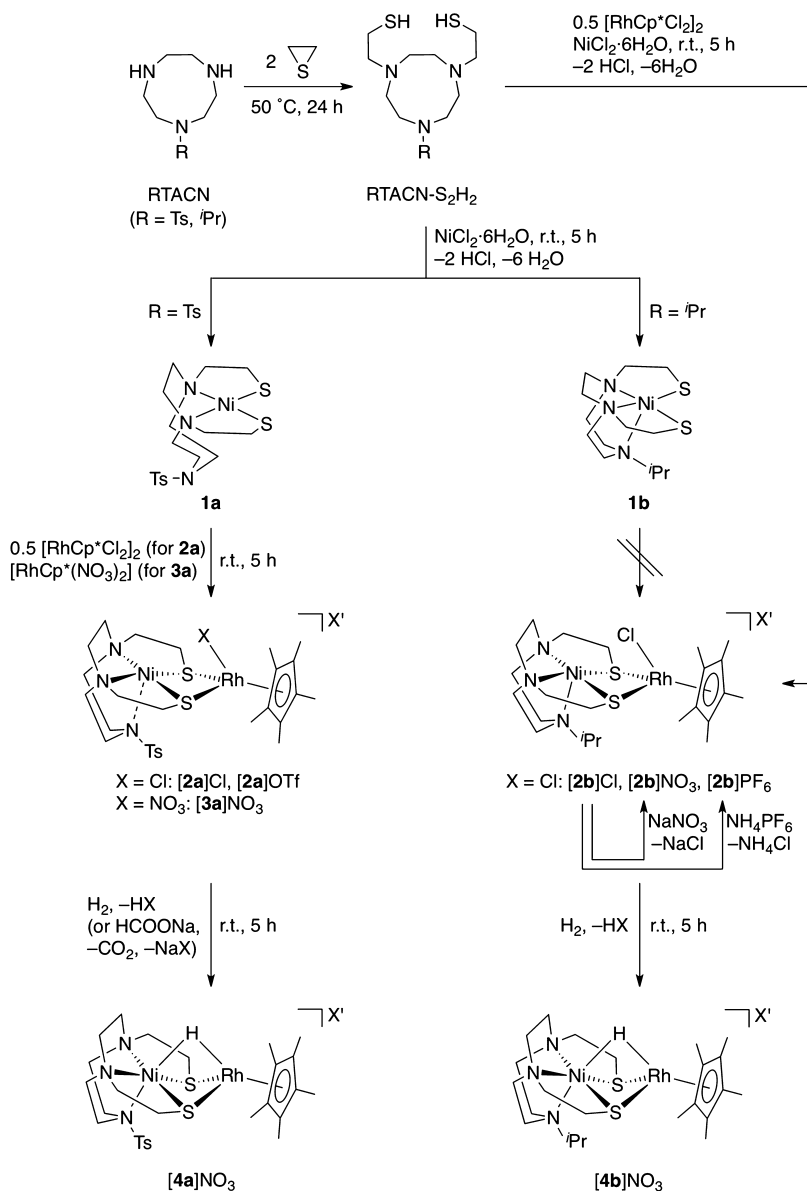
Received: April 27, 2012

Published: June 26, 2012

Chart 1



Scheme 1



atom was crucial for its catalytic activity. When the OH ligand was protonated at low pH, the corresponding NiRu hydride lost its reducing ability.¹⁰ Although the detailed structure of the active NiRu complex is not yet determined, these results suggested that the tuning of the Ni^{II} electronic state is very important to developing water-soluble $[\text{NiFe}]$ hydrogenase-mimicking catalysts.

In the present study, we have developed new water-soluble bis(μ -thiolato)(μ -hydrido) Ni^{III}Rh^{III} dinuclear complexes, $[(\text{RTACN-S}_2)\text{Ni}(\mu\text{-H})\text{RhCp}^*]\text{NO}_3$ ($\text{RTACN-S}_2\text{H}_2 = 1,4$ -bis-

(2-mercaptoethyl)-7-R-1,4,7-triazacyclononane; $\text{R} = p$ -toluenesulfonyl (Ts) ($[\text{4a}]\text{NO}_3$) and isopropyl (iPr) ($[\text{4b}]\text{NO}_3$)) (Scheme 1), which were inspired from the active site of $[\text{NiFe}]$ hydrogenases to tune the electronic state of the Ni^{II} center by varying the substituent group of the pendant amino group. By introducing an electron-withdrawing Ts group onto the amino nitrogen *trans* to the hydride, the hydride-bridged Ni^{II}Rh^{III} complex ($[\text{4a}]\text{NO}_3$) was significantly stabilized in water, and consequently, we found out its efficiency to promote hydrogenation of aldehydes and CO₂ in aqueous media. We

wish to report herein the synthesis and characterization of hydride-bridged $\text{Ni}^{\text{II}}\text{Rh}^{\text{III}}$ complexes by designing the new N_3S_2 dithiolato ligands and their catalytic activities for hydrogenation of the carbonyl compounds in water.

EXPERIMENTAL SECTION

Materials. All preparative procedures were carried out under a nitrogen atmosphere in a glovebox or using standard Schlenk techniques. All chemicals (highest purity available) were purchased from Wako Pure Chemical Industries, Ltd. Reagent grade solvents were dried by the standard procedures and were freshly distilled prior to its use. CO_2 (>99.99%) and H_2 (>99.999%) gases were purchased from Sumitomo Seika Co., Ltd. Compounds, 1-(*p*-toluenesulfonyl)-1,4,7-triazacyclononane,^{11a,b} 1-isopropyl-1,4,7-triazacyclononane,^{11c} $[\text{RhCp}^*\text{Cl}_2]_2$,^{11d} and $\text{RhCp}^*(\text{NO}_3)_2$ ^{11e} were prepared by the methods described in the literature. The pH of the aqueous solution was adjusted by using 0.1 M $\text{HNO}_3/\text{H}_2\text{O}$ (pH 1–3), 25 mM $\text{CH}_3\text{COOH}/\text{CH}_3\text{COONa}$ (pH 4–6), 25 mM $\text{Na}_2\text{HPO}_4/\text{KH}_2\text{PO}_4$ (pH 7–8), and 0.1 M $\text{NaOH}/\text{H}_2\text{O}$ (pH 9–12) solutions.

Measurements. ^1H NMR spectra were recorded on a Bruker 300 MHz spectrometer (AV-300N). The ^1H NMR spectra in CDCl_3 or CD_3CN were reported in parts per million versus tetramethylsilane (TMS) as an external reference, and those in D_2O or H_2O were performed by dissolving samples in D_2O or H_2O in an NMR tube (diameter = 5.0 mm) with a sealed capillary tube (diameter = 1.5 mm) containing 3-(trimethylsilyl)propionic-2,2,3,3- d_4 acid sodium salt (TSP) in D_2O (10 mM) as an internal reference. IR spectra of solid compounds, as KBr disks, were recorded on a JASCO FT/IR-410 spectrophotometer at ambient temperature. ESI-TOF mass spectra were recorded on a JEOL JMS-T100LC in a positive detection mode in the range of m/z 100–2000, equipped with an ion spray interface. The sprayer was held at a potential of +2.0 kV, and the compressed N_2 was employed to assist liquid nebulization. The orifice potential was maintained at +20 V. The pH of the solution was determined by a pH meter (model: TOA WM-22EP) equipped with a glass electrode (model: TOA GST-2729C), and the pD values were corrected by adding 0.4 to the observed values.¹²

1,4-Bis(2-mercaptoethyl)-7-(*p*-toluenesulfonyl)-1,4,7-triazacyclononane ($\text{TsTACN-S}_2\text{H}_2$). To a solution of 1-(*p*-toluenesulfonyl)-1,4,7-triazacyclononane (TsTACN , 500 mg, 1.76 mmol) in dry chloroform (20 mL) was added ethylene sulfide (0.7 mL, 11.8 mmol) at room temperature, and the mixture was stirred at 50 °C for 24 h. The excess ethylene sulfide and solvent were removed under reduced pressure to give the product $\text{TsTACN-S}_2\text{H}_2$, which was used for preparation of **1a** without further purification. Yield: 673 mg, 95% (vs TsTACN). ^1H NMR (300 MHz, CDCl_3): δ 2.42 (s, 3H, $\text{CH}_3(\text{Ts})$), 2.54–2.62 (m, 4H, $-\text{CH}_2-$), 2.64–2.82 (m, 8H, $-\text{CH}_2-$), 2.95–2.98 (m, 4H, $-\text{CH}_2-$), 3.26–3.29 (m, 4H, $-\text{CH}_2-$), 7.30 (d, $^3J_{\text{HH}} = 8.3$ Hz, 2H, $\text{ArH}(\text{Ts})$), 7.66 (d, $^3J_{\text{HH}} = 8.1$ Hz, 2H, $\text{ArH}(\text{Ts})$). $^{13}\text{C}\{^1\text{H}\}$ NMR (75 MHz, CDCl_3): δ 21.5 ($\text{CH}_3(\text{Ts})$), 23.1 ($\text{CH}_2-\text{CH}_2-\text{SH}$), 51.3 ($-\text{CH}_2-(\text{TACN})$), 55.8 ($\text{CH}_2-\text{CH}_2-\text{SH}$), 56.2 ($-\text{CH}_2-(\text{TACN})$), 61.0 ($-\text{CH}_2-(\text{TACN})$), 127.3 ($-\text{CH}-(\text{Ts})$), 129.8 ($-\text{CH}-(\text{Ts})$), 136.0 ($\text{C}-\text{SO}_2-(\text{Ts})$), 143.3 ($\text{C}-\text{CH}_3(\text{Ts})$). ESI-MS (in MeOH): m/z 404.15 ($I = 100\%$) ($z = 1$, $[\text{TsTACN-S}_2\text{H}_2 + \text{H}]^+$ (404.15)). IR (KBr): ν 2925, 2850, 2574 (SH), 1598, 1449, 1335, 1158, 916, 816, 713, 694, 642, 549 cm^{-1} .

1,4-Bis(2-mercaptoethyl)-7-isopropyl-1,4,7-triazacyclononane ($^i\text{PrTACN-S}_2\text{H}_2$). To a solution of 1-isopropyl-1,4,7-triazacyclononane ($^i\text{PrTACN}$, 222 mg, 1.30 mmol) in dry benzene (10 mL) was added ethylene sulfide (9 mL, 151 mmol) at room temperature, and the mixture was stirred at 50 °C for 24 h. The excess ethylene sulfide and solvent were removed under reduced pressure to give the product $^i\text{PrTACN-S}_2\text{H}_2$, which was used for the preparation of **1b** and **[2b]Cl** without further purification. Yield: 334 mg, 88% (vs $^i\text{PrTACN}$). ^1H NMR (300 MHz, CDCl_3): δ 0.97 (d, $^3J_{\text{HH}} = 6.5$ Hz, 6H, $\text{CH}_3(^i\text{Pr})$), 2.56–2.90 (m, 21H). $^{13}\text{C}\{^1\text{H}\}$ NMR (75 MHz, CDCl_3): δ 18.3 ($-\text{CH}(\text{CH}_3)_2$), 23.4 ($\text{CH}_2-\text{CH}_2-\text{SH}$), 52.4 ($-\text{CH}_2-(\text{TACN})$), 54.8 ($-\text{CH}(\text{CH}_3)_2$), 55.9 ($-\text{CH}_2-(\text{TACN})$), 56.4 ($-\text{CH}_2-(\text{TACN})$), 61.4 ($\text{CH}_2-\text{CH}_2-\text{SH}$). ESI-MS (in CHCl_3): m/z 291.99 ($I =$

100%) ($z = 1$, $[\text{PrTACN-S}_2\text{H}_2 + \text{H}]^+$ (292.18)). IR (KBr): ν 2960, 2925, 2802, 2545 ($-\text{SH}$), 1459, 1380, 1358, 1310, 1116, 1099 cm^{-1} .

[Ni(TsTACN-S_2)] (1a**).** A solution of $\text{NiCl}_2 \cdot 6\text{H}_2\text{O}$ (755 mg, 3.18 mmol) in methanol (60 mL) was slowly added to a solution of $\text{TsTACN-S}_2\text{H}_2$ (1.42 g, 3.53 mmol) in chloroform (40 mL) under N_2 . The mixture was stirred at room temperature for 5 h to yield a brown solution, which was evaporated to dryness. The crude product was purified by chromatography on an alumina column (Wako, alumina, activated particle size = 40–150 μm) with chloroform and methanol (95:5) as the eluent. The first purple band was collected, and the solvent was removed by rotary evaporation. The resultant purple oil was dissolved in acetonitrile (20 mL) and was stored for 12 h at room temperature to afford a purple solid, which was filtered and washed with acetonitrile and diethyl ether. Yield: 588 mg, 40% (vs $\text{NiCl}_2 \cdot 6\text{H}_2\text{O}$). ^1H NMR (300 MHz, CDCl_3): δ 2.28–2.46 (m, 4H, $-\text{CH}_2-$), 2.48 (s, 3H, $\text{CH}_3(\text{Ts})$), 2.70–2.86 (m, 6H, $-\text{CH}_2-$), 3.09–3.19 (m, 2H, $-\text{CH}_2-$), 3.46–3.57 (m, 2H, $-\text{CH}_2-$), 3.67–3.77 (m, 2H, $-\text{CH}_2-$), 4.13–4.20 (m, 2H, $-\text{CH}_2-$), 5.90–6.05 (m, 2H, $-\text{CH}_2-$), 7.39 (d, $^3J_{\text{HH}} = 8.1$ Hz, 2H, $\text{ArH}(\text{Ts})$), 7.75 (d, $^3J_{\text{HH}} = 8.3$ Hz, 2H, $\text{ArH}(\text{Ts})$). $^{13}\text{C}\{^1\text{H}\}$ NMR (75 MHz, CDCl_3): δ 21.7 ($\text{CH}_3(\text{Ts})$), 28.4 ($\text{CH}_2-\text{CH}_2-\text{SH}$), 56.2 ($-\text{CH}_2-(\text{TACN})$), 60.2 ($-\text{CH}_2-(\text{TACN})$), 61.3 ($-\text{CH}_2-(\text{TACN})$), 66.6 ($\text{CH}_2-\text{CH}_2-\text{S}$), 127.1 ($-\text{CH}-(\text{Ts})$), 130.3 ($-\text{CH}-(\text{Ts})$), 135.1 ($\text{C}-\text{SO}_2-(\text{Ts})$), 144.6 ($\text{C}-\text{CH}_3(\text{Ts})$). ESI-MS (in MeOH): m/z 481.88 ($I = 100\%$) ($z = 1$, $[(\text{1a} + \text{Na})]^+$ (482.05)). IR (KBr): ν 2942, 2886, 2840, 1596, 1449, 1435, 1333, 1318, 1158, 1089, 1001, 957, 922, 849, 813, 713, 693, 643, 545 cm^{-1} . Anal. Calcd for $\text{C}_{17}\text{H}_{27}\text{N}_3\text{NiO}_2\text{S}_3$: C, 44.36; H, 5.91; N, 9.13. Found: C, 44.46; H, 5.69; N, 9.07. Purple-green crystals of **1a** used for an X-ray analysis were obtained from a DMF/diethyl ether solution.

[Ni($^i\text{PrTACN-S}_2$)] (1b**).** A solution of $\text{NiCl}_2 \cdot 6\text{H}_2\text{O}$ (570 mg, 2.40 mmol) in methanol (30 mL) was slowly added to a solution of $^i\text{PrTACN-S}_2\text{H}_2$ (969 mg, 2.40 mmol) in chloroform (10 mL) under N_2 . The mixture was stirred at room temperature for 5 h to yield a brown solution, which was evaporated to dryness. The crude product was purified by chromatography on an alumina column (Wako, alumina, activated particle size = 40–150 μm) with chloroform and methanol (95:5) as the eluent. The first green band was collected, and the solvent was removed by rotary evaporation. The green residue was washed with toluene and diethyl ether and recrystallized from CH_2Cl_2 /diethyl ether to give a green powder of **1b**. Yield: 170 mg, 20% (vs $\text{NiCl}_2 \cdot 6\text{H}_2\text{O}$). ESI-MS (in MeOH): m/z 346.98 ($I = 100\%$) ($z = 1$, $[\text{1b}]^+$ (347.10)). IR (KBr): ν 2917, 1635, 1458, 1261, 1085, 810 cm^{-1} . Anal. Calcd for $\text{C}_{16.5}\text{H}_{35}\text{Cl}_3\text{N}_3\text{NiO}_{0.5}\text{S}_2$ (**1b**·1.5 CH_2Cl_2 ·0.5 Et_2O): C, 38.66; H, 6.88; N, 8.20. Found: C, 38.56; H, 6.56; N, 8.58. Green crystals of **1b** for an X-ray analysis were obtained from a dichloromethane/diethyl ether solution.

[Ni(TsTACN-S_2)RhCp*Cl]X' ([2a]X'**; X' = Cl and OTf).** Complex **1a** (206 mg, 0.448 mmol) was reacted with $[\text{RhCp}^*\text{Cl}_2]_2$ (138 mg, 0.224 mmol) in dichloromethane (100 mL) at room temperature for 5 h to provide a red solution, from which a red powder of **[2a]Cl** was obtained by removing the solvent. Yield: 341 mg, 99%. ^1H NMR (300 MHz, CDCl_3): δ 1.66 (s, 15H, $\text{CH}_3(\text{Cp}^*)$), 2.48 (s, 3H, $\text{CH}_3(\text{Ts})$), 2.00–2.06, 2.54–2.74, 3.09–4.15 (m, 20H), 7.41 (d, $^3J_{\text{HH}} = 8.1$ Hz, 2H, $\text{ArH}(\text{Ts})$), 7.84 (d, $^3J_{\text{HH}} = 8.3$ Hz, 2H, $\text{ArH}(\text{Ts})$). ESI-MS (in MeOH): m/z 731.82 ($I = 100\%$) ($z = 1$, $[\text{2a}]^+$ (732.05)). IR (KBr): ν 2914, 1625, 1491, 1455, 1340, 1162, 1087, 926, 752, 712, 694, 572, 548 cm^{-1} . Anal. Calcd for $\text{C}_{27.5}\text{H}_{43}\text{Cl}_3\text{N}_3\text{NiO}_2\text{RhS}_3$ (**[2a]**·Cl·0.5 CH_2Cl_2): C, 40.69; H, 5.34; N, 5.18. Found: C, 40.48; H, 5.26; N, 5.31. Addition of NH_4OTf (200 mg, 1.20 mmol) to an aqueous solution (20 mL) of **[2a]Cl** (350 mg, 0.455 mmol) gave a red precipitate of **[2a]OTf**, which was filtered, washed with H_2O and diethyl ether, and dried in vacuo. Yield: 360 mg, 91%. ^1H NMR (300 MHz, CDCl_3): δ 1.67 (s, 15H, $\text{CH}_3(\text{Cp}^*)$), 2.50 (s, 3H, $-\text{CH}_3(\text{Ts})$), 2.01–2.06, 2.45–3.16, 3.77–4.05 (m, 20H), 7.44 (d, $^3J_{\text{HH}} = 8.1$ Hz, 2H, $\text{ArH}(\text{Ts})$), 7.85 (d, $^3J_{\text{HH}} = 8.2$ Hz, 2H, $\text{ArH}(\text{Ts})$). ESI-MS (in MeOH): m/z 731.90 ($I = 100\%$) ($z = 1$, $[\text{2a}]^+$ (732.05)). IR (KBr): ν 2919, 1628, 1457, 1278, 1160, 1031, 694, 639 cm^{-1} . Anal. Calcd for $\text{C}_{28}\text{H}_{42}\text{ClF}_3\text{N}_3\text{NiO}_3\text{RhS}_4$: C, 38.09; H, 4.79; N, 4.76. Found: C, 37.71; H, 4.73; N, 4.71. Red crystals of **[2a]OTf**· Et_2O suitable for X-ray

crystallography were obtained from a CH_2Cl_2 solution of $[\mathbf{2a}]\text{OTf}$ layered with diethyl ether at 4 °C.

$[\text{Ni}(\text{PrTACN-S}_2)\text{RhCp}^*\text{Cl}]\text{X}'$ ($[\mathbf{2b}]\text{X}'$: $\text{X}' = \text{Cl}$, NO_3 , and PF_6). A methanolic solution (40 mL) of $\text{NiCl}_2 \cdot 6\text{H}_2\text{O}$ (184 mg, 0.773 mmol) was slowly added to a solution of $\text{PrTACN-S}_2\text{H}_2$ (0.773 mmol) in CHCl_3 (4 mL). After stirring for 1 h, a solution of $[\text{RhCp}^*\text{Cl}_2]_2$ (240 mg, 0.388 mmol) in CHCl_3 (40 mL) was added to the mixture, which was stirred for 4 h. The solvent was removed to dryness, and the resulting dark brown oil was extracted with CH_3CN (100 mL). The orange extract was filtered and evaporated to dryness. The crude product was purified by chromatography on an alumina column (Wako, alumina, activated particle size = 40–150 μm) and eluted with chloroform and methanol (95:5). The first orange band was collected, and the solvent was removed by rotary evaporation. The resultant red oil was recrystallized from CH_2Cl_2 /diethyl ether to give a dark red powder of $[\mathbf{2b}]\text{Cl}$. Yield: 140 mg, 28% (vs $\text{PrTACN-S}_2\text{H}_2$). ESI-MS (in MeOH): m/z 619.95 ($I = 100\%$) ($z = 1$, $[\mathbf{2b}]^+$ (620.09)). IR (KBr): ν 2912, 2852, 1652, 1495, 1448, 1377, 1288, 1271, 1084, 1062, 1029, 1010, 977, 755, 720 cm^{-1} . Anal. Calcd for $\text{C}_{23.5}\text{H}_{43.3}\text{Cl}_3\text{NiRhS}_2$ ($[\mathbf{2b}]\text{Cl} \cdot 0.5\text{CH}_2\text{Cl}_2$): C, 40.34; H, 6.19; N, 6.01. Found: C, 40.18; H, 6.30; N, 6.25. A solution of $[\mathbf{2b}]\text{Cl}$ (210 mg, 0.320 mmol) in 50 mL of H_2O was loaded onto a Dowex 1-X8 column (NO_3^- form, 100–200 mesh) and eluted with water. The eluate was evaporated to give a red powder of $[\mathbf{2b}]\text{NO}_3$, which was dried in vacuo. Yield: 216 mg, 99%. ESI-MS (in MeOH): m/z 619.94 ($I = 100\%$) ($z = 1$, $[\mathbf{2b}]^+$ (620.09)). IR (KBr): ν 2970, 2916, 2852, 1663, 1384 (NO_3^-), 1360, 1084, 1021, 830 cm^{-1} . Complex $[\mathbf{2b}]\text{NO}_3$ is very hygroscopic, preventing satisfactory elemental analysis results. Addition of NH_4PF_6 (50 mg, 0.307 mmol) to an aqueous solution (10 mL) of $[\mathbf{2b}]\text{Cl}$ (18 mg, 27.4 μmol) gave a red powder. The crude product was collected by filtration, washed with water and diethyl ether, and recrystallized from CH_2Cl_2 /diethyl ether to give $[\mathbf{2b}]\text{PF}_6$ as a dark red powder. Yield: 12 mg, 57%. ^1H NMR (300 MHz, CD_3CN): δ 1.56 (s, $\text{CH}_3(\text{Cp}^*)$) ppm. ESI-MS (in MeOH): m/z 619.93 ($I = 100\%$) ($z = 1$, $[\mathbf{2b}]^+$ (620.09)). IR (KBr): ν 2973, 2918, 2851, 1633, 1498, 1456, 1399, 1385, 1300, 839, 558 cm^{-1} . Anal. Calcd for $\text{C}_{23.5}\text{H}_{43.3}\text{Cl}_2\text{F}_6\text{NiRhS}_2$ ($[\mathbf{2b}]\text{PF}_6 \cdot 0.5\text{CH}_2\text{Cl}_2$): C, 34.88; H, 5.36; N, 5.19. Found: C, 34.96; H, 5.13; N, 5.29. Red crystals of $[\mathbf{2b}]\text{PF}_6$ suitable for X-ray crystallography were obtained from a mixed solvent of acetonitrile/diethyl ether.

$[\text{Ni}(\text{TsTACN-S}_2)\text{RhCp}^*\text{NO}_3]\text{NO}_3$ ($[\mathbf{3a}]\text{NO}_3$). Reaction of $\mathbf{1a}$ (129 mg, 0.280 mmol) with $[\text{RhCp}^*(\text{NO}_3)_2]$ (101 mg, 0.279 mmol) in methanol (40 mL) at room temperature for 5 h provided a red solution. After filtration, the solvent was removed under reduced pressure to yield a red powder of $[\mathbf{3a}]\text{NO}_3$. Yield: 230 mg, 99% (vs $\mathbf{1a}$). ^1H NMR (300 MHz, D_2O): δ 1.70 (s, 15H, $\text{CH}_3(\text{Cp}^*)$), 2.51 (s, 3H, $-\text{CH}_3(\text{Ts})$), 2.43–2.49, 2.61–2.88, 2.90–3.03, 3.36–3.80, 4.16–4.35 (m, 20H), 7.61 (d, $^3J_{\text{HH}} = 8.3$ Hz, 2H, $\text{ArH}(\text{Ts})$), 7.98 (d, $^3J_{\text{HH}} = 8.3$ Hz, 2H, $\text{ArH}(\text{Ts})$). ESI-MS (in $\text{H}_2\text{O}/\text{MeOH} = 9:1$): m/z 758.94 ($I = 100\%$) ($z = 1$, $[\mathbf{3a}]^+$ (759.07)). IR (KBr): ν 2915, 2855, 1458, 1384, 1352, 1325, 1274, 1164, 713, 693, 548 cm^{-1} . Anal. Calcd for $\text{C}_{27}\text{H}_{42}\text{N}_3\text{NiO}_8\text{RhS}_3$: C, 39.43; H, 5.15; N, 8.52. Found: C, 39.04; H, 4.93; N, 8.38. Red crystals of $[\mathbf{3a}]\text{NO}_3$ suitable for X-ray crystallography were obtained from a MeOH/diethyl ether solution.

$[(\text{TsTACN-S}_2)\text{Ni}(\mu\text{-H})\text{RhCp}^*]\text{NO}_3$ ($[\mathbf{4a}]\text{NO}_3$). Method A: Complex $[\mathbf{3a}]\text{NO}_3$ (38 mg, 46 μmol) was dissolved in a phosphate buffer solution (pH 7, 25 mM, 2 mL), and H_2 gas (0.1 MPa) was bubbled through the solution at room temperature. The reaction mixture was stirred for 5 h to afford a very air-sensitive dark red precipitate of $[\mathbf{4a}]\text{NO}_3$, which was filtered off. Yield: 24 mg, 67%. Brown crystals of $[\mathbf{4a}]\text{NO}_3 \cdot 1.5\text{H}_2\text{O}$ suitable for X-ray crystallography were obtained from a mixed solvent of MeOH/diethyl ether at 4 °C. Method B: Complex $[\mathbf{3a}]\text{NO}_3$ (21 mg, 26 μmol) was treated with HCOONa (46 mg, 0.676 mmol) in H_2O (1 mL) at pH 7 at room temperature for 5 h to yield a dark red powder of $[\mathbf{4a}]\text{NO}_3$, which was filtered and dried in vacuo. Yield: 9 mg, 48% (vs $[\mathbf{3a}]\text{NO}_3$). ESI-MS (in MeOH): m/z 697.99 ($I = 100\%$) ($z = 1$, $[\mathbf{4a}]^+$ (698.09)). IR (KBr): ν 2912, 1923 (M–H), 1635, 1597, 1456, 1384, 1362, 1167, 1083, 691 cm^{-1} . Anal. Calcd for $\text{C}_{30.5}\text{H}_{46.5}\text{N}_4\text{Na}_{0.5}\text{NiO}_{12}\text{RhS}_3$ ($[\mathbf{4a}]\text{NO}_3 \cdot 3.5\text{HCOONa}$): C, 36.65; H, 4.69; N, 5.61. Found: C, 36.67; H, 4.81; N, 5.94. The sample for elemental analysis was prepared by Method B and contained an

impurity of 3.5 equiv of HCOONa , which was confirmed by ^1H NMR spectroscopy with TSP as an internal standard.

$[(\text{PrTACN-S}_2)\text{Ni}(\mu\text{-H})\text{RhCp}^*]\text{NO}_3$ ($[\mathbf{4b}]\text{NO}_3$). By a procedure similar to Method A for $[\mathbf{4a}]\text{NO}_3$, a dark red powder of $[\mathbf{4b}]\text{NO}_3$ was obtained from $[\mathbf{2b}](\text{NO}_3)$ (21 mg, 30.7 μmol). Yield: 2 mg, 10%. ESI-MS (in $\text{H}_2\text{O}/\text{MeOH} = 9:1$): m/z 585.98 ($I = 100\%$) ($z = 1$, $[\mathbf{4b}]^+$ (586.13)). IR (KBr): ν 2952, 2912, 2852, 1937 (M–H), 1634, 1493, 1456, 1385, 1290, 1082, 759 cm^{-1} . Anal. Calcd for $\text{C}_{23}\text{H}_{44}\text{Cl}_{0.5}\text{Na}_{0.5}\text{NiO}_{3.5}\text{RhS}_2$ ($[\mathbf{4b}]\text{NO}_3 \cdot 0.5\text{NaCl} \cdot 0.5\text{H}_2\text{O}$): C, 40.18; H, 6.45; N, 8.15. Found: C, 39.83; H, 6.14; N, 8.25. The contamination of NaCl in the sample was assumed to be derived from the phosphate buffer solution ($\text{NaH}_2\text{PO}_4/\text{Na}_2\text{HPO}_4$) and $[\mathbf{2b}](\text{NO}_3)$. Dark red crystals of $[\mathbf{4b}]\text{NO}_3 \cdot 1.5\text{H}_2\text{O}$ suitable for X-ray crystallography were obtained from an aqueous solution of $[\mathbf{4b}]\text{NO}_3$ at room temperature.

Typical Procedure for Hydrogenations of Aldehydes and CO_2 in Aqueous Solutions Catalyzed by Dinuclear NiRh Complexes. Benzaldehyde (250 μmol) and $[\mathbf{3a}]\text{NO}_3$ (5 μmol) were dissolved in an aqueous phosphate buffer solution (2 mL, pH 7) under H_2 (0.1 MPa), and the mixture was vigorously stirred at 60 °C. After 1 h, the reaction solution was quickly cooled with an ice bath and was analyzed by ^1H NMR spectroscopy to determine the initial turnover frequencies (TOFs). The yields were similarly determined from the same reactions after 12 h. Complex $[\mathbf{3a}]\text{NO}_3$ (5 μmol) was dissolved in an aqueous phosphate buffer solution (5 mL, pH 7) in a pressure vessel, and the solution was charged with CO_2 (1 MPa) and H_2 (1 MPa). After stirring for 20 h at 20 °C, the pressure was released and the solution was quickly cooled with an ice bath. The yield of HCOONa was determined by ^1H NMR measurements with TSP as an internal standard. The HCOO^- signal was observed at 8.41 ppm at pH 7. Blank experiments showed that no hydrogenation occurred in the absence of $[\mathbf{3a}]\text{NO}_3$.

X-ray Crystallographic Analyses. Crystallographic and experimental data for $\mathbf{1a}$, $\mathbf{1b}$, $[\mathbf{2a}]\text{OTf} \cdot \text{Et}_2\text{O}$, $[\mathbf{2b}]\text{PF}_6$, $[\mathbf{3a}]\text{NO}_3$, $[\mathbf{4a}]\text{NO}_3 \cdot 1.5\text{H}_2\text{O}$, and $[\mathbf{4b}]\text{NO}_3 \cdot 1.5\text{H}_2\text{O}$ are listed in Tables S1–S3 (see the Supporting Information). Measurements were carried out on a Rigaku AFC8R/Mercury CCD diffractometer equipped with graphite-monochromated Mo $K\alpha$ radiation (0.71075 Å) using a rotating-anode X-ray generator (50 kV, 170 mA) and a Rigaku VariMax Mo/Saturn CCD diffractometer equipped with graphite-monochromated Mo $K\alpha$ radiation using a rotating-anode X-ray generator RA-Micro7 (50 kV, 24 mA). A total of 2160 oscillation images, covering a whole sphere of $6^\circ < 2\theta < 55^\circ$, were corrected by the ω -scan method with $\Delta\omega = 0.25^\circ$. The crystal-to-detector (70 \times 70 mm) distance was set at 60 mm. The data were processed using the Crystal Clear 1.3.5 program (Rigaku/MSU)¹³ and corrected for Lorentz-polarization and absorption effects.¹⁴ The structures of complexes were solved by direct methods with SHELX-97¹⁵ ($[\mathbf{2b}]\text{PF}_6$), SIR-92¹⁶ ($\mathbf{1a}$, $[\mathbf{4a}]\text{NO}_3$) and SIR-97¹⁶ ($\mathbf{1b}$, $[\mathbf{2a}]\text{OTf}$, $[\mathbf{3a}]\text{NO}_3$, $[\mathbf{4b}]\text{NO}_3$) and were refined on F^2 with full-matrix least-squares techniques with SHELXL-97¹⁵ using the Crystal Structure 4.0 package.¹⁷ All non-hydrogen atoms (except the disordered nitrate anion of $[\mathbf{4b}]\text{NO}_3$) were refined with anisotropic thermal parameters, and the C–H hydrogen atoms were calculated at ideal positions and refined with riding models. The hydride H atoms of $[\mathbf{4a}]\text{NO}_3$ (H1, H2) and $[\mathbf{4b}]\text{NO}_3$ (H1) were determined from difference Fourier maps and were refined isotropically. In the structure of $[\mathbf{3a}]\text{NO}_3$, the coordinated nitrate anion was disordered and refined with two site pivoting models (N41O32O4O5 and N42O31O4O6), each having 0.5 occupancy with the O4 atom on the pivot axis with 1.0 occupancy. Both of the disordered NO_3^- fragments were constrained to be planar and were refined anisotropically. In the structure of $[\mathbf{4b}]\text{NO}_3$, the counteranion of NO_3^- was disordered at a special position (N4O1O2O3) and around another special position (N5O4O5O6) with each being 0.5 occupancy. The former nitrate was refined anisotropically, and the latter was constrained as a planar rigid model with isotropic thermal parameters. All calculations were carried out on a Pentium PC with the Crystal Structure 4.0 package.¹⁷

RESULTS AND DISCUSSION

N₃S₂ Dithiolato Ligands RTACN-S₂H₂ (R = Ts, ⁱPr). New ligands, 1,4-bis(2-mercaptoethyl)-7-R-1,4,7-triazacyclononane (RTACN-S₂H₂; R = Ts, ⁱPr), were designed to prepare a Ni^{II} center having three Ni–N and two Ni–S bonds with a potential one vacant coordination site. In addition to the ability of dithiolato units to bridge an additional metal, the vacant coordination site should be readily occupied by exogenous substrates, and furthermore, the electronic state of the Ni center can be controlled by changing the substituent R on the TACN ligand. In pioneering papers, the syntheses of TACN-based ligands with one, two, and three thiol pendants and the corresponding mononuclear and homometallic dinuclear complexes have been reported.¹⁸ In this work, we have constructed Ni^{II}Rh^{III} heterodinuclear centers in stepwise fashion by using RTACN-S₂H₂ ligands (R = Ts, ⁱPr), which were synthesized from the reactions of RTACN with ethylene sulfide in high yields (Scheme 1).

Mononuclear Ni Complexes [Ni(RTACN-S₂)] (R = Ts (1a), ⁱPr (1b)). The mononuclear Ni complexes **1a** and **1b** were prepared from the reactions of RTACN-S₂H₂ (R = Ts (**1a**), ⁱPr (**1b**)) with NiCl₂·6H₂O in mixed solvents of CHCl₃/methanol. The Ni1 atom of **1a** has a square-planar coordination geometry with bonding parameters that are usual for the previously reported Ni^{II}N₂S₂(thiolato) complexes (Figure 1a).¹⁹ The distances between Ni1 and the nitrogen

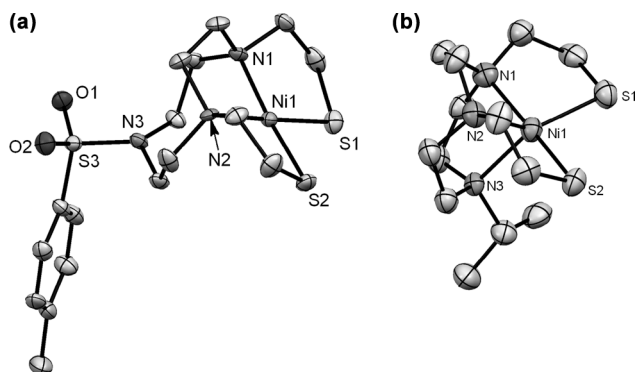


Figure 1. (a) ORTEP drawing of **1a**. Hydrogen atoms are omitted for clarity. Selected distances (Å) and angles (deg): Ni1–S1 = 2.1632(14), Ni1–S2 = 2.1698(10), Ni1–N1 = 1.965(3), Ni–N2 = 1.973(4), Ni1–N3 = 3.423(4), S1–Ni1–S2 = 93.54(5), S1–Ni1–N1 = 90.38(11), S1–Ni1–N2 = 178.09(7), S2–Ni1–N1 = 170.11(9), S2–Ni1–N2 = 88.35(8), N1–Ni1–N2 = 87.70(13). (b) ORTEP drawing of **1b**. Selected distances (Å) and angles (deg): Ni1–S1 = 2.318(5), Ni1–S2 = 2.418(5), Ni1–N1 = 2.224(9), Ni–N2 = 2.133(8), Ni1–N3 = 2.207(8), S1–Ni1–S2 = 97.11(13), S1–Ni1–N1 = 88.2(3), S1–Ni1–N2 = 141.3(3), S1–Ni1–N3 = 131.1(3), S2–Ni1–N1 = 170.1(2), S2–Ni1–N2 = 86.9(3), N1–Ni1–N2 = 83.7(3).

atoms of the TACN ligand are not equivalent, wherein the distance of Ni1–N3 (3.423(4) Å) is quite longer than those of Ni1–N1 and Ni–N2 (1.965(3) and 1.973(4) Å), suggesting no interaction between the Ni1 and N3 atoms since the basicity of the N3 amino group is considerably reduced, owing to the electron-withdrawing Ts group. In contrast to the traditional Ni^{II}N₂S₂ complexes and **1a**, the Ni1 atom of **1b** has a distorted trigonal-bipyramidal geometry (τ value = 0.48)²⁰ with a normal coordination of the N3 atom possessing an electron-donating ⁱPr group (Figure 1b). The S2 and N1 atoms occupy the axial positions, whereas the S1, N2, and N3 atoms are in the

equatorial ones. The ¹H NMR spectrum of **1a** showed sharp signals, and in contrast, that of **1b** exhibited only broad featureless signals, which is consistent with a high-spin Ni(II) state.

Dinuclear NiRh Complexes [Ni(TsTACN-S₂)RhCp*X]X' (X = Cl, X' = Cl, OTf ([2a]X'); X = X' = NO₃ ([3a]NO₃)) and [Ni(ⁱPrTACN-S₂)RhCp*Cl]X' (X' = Cl, NO₃, PF₆ ([2b]X')). The dithiolato-bridged Ni^{II}Rh^{III} dinuclear complex [Ni(TsTACN-S₂)RhCp*Cl]Cl ([2a]Cl) was prepared by reacting **1a** with 0.5 equiv of [RhCp*Cl₂]₂ in dichloromethane and was further converted by treatment with NH₄OTf in water to a red powder of [2a]OTf quantitatively. When **1a** was reacted with an equimolar amount of [RhCp*(NO₃)₂] in methanol, [Ni(TsTACN-S₂)RhCp*(NO₃)]NO₃ ([3a]NO₃) was obtained in high yield. Complexes [2a]X' (X' = Cl, OTf) and [3a]NO₃ were characterized by ¹H NMR, ESI-MS (Figure S2 for [2a]OTf and Figure S4 for [3a]NO₃ in the Supporting Information), IR, and elemental analysis. The IR spectrum of [3a]NO₃ (Figure S7, Supporting Information) showed peaks at 1384 cm^{−1} as well as at 1458 and 1274 cm^{−1}. The former peak is attributable to a free NO₃[−] anion, and the latter two are assignable to a coordinating NO₃[−] ligand in a monodentate fashion.²¹ Complexes [2a]Cl and [3a]NO₃ have high solubility in H₂O ([2a]Cl, 30 mg/mL; [3a]NO₃, 21 mg/mL at 20 °C) and were stable in water in a range of pH 1–11, which were confirmed by ¹H NMR spectra.

ORTEP drawings for the complex cations of [2a]OTf and [3a]NO₃ are shown in Figure 2 and Figure S1 (Supporting

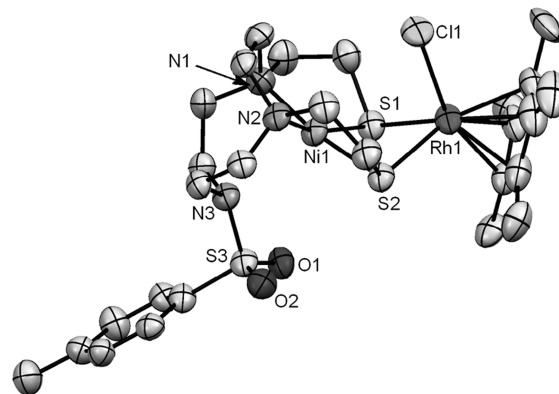


Figure 2. ORTEP drawing of [2a]OTf. The counteranion (OTf) and hydrogen atoms are omitted for clarity. Selected distances (Å) and angles (deg): Ni1–Rh1 = 3.207(2), Ni1–S1 = 2.173(3), Ni1–S2 = 2.164(3), Ni1–N1 = 1.959(7), Ni1–N2 = 1.977(6), Ni1–N3 = 2.614(7), Rh1–S1 = 2.414(3), Rh1–S2 = 2.395(3), Rh1–Cl1 = 2.412(3), Ni1–S1–Rh1 = 89.26(8), Ni1–S2–Rh1 = 88.54(8).

Information). The complex cation of [2a]OTf is composed of Ni^{II}Rh^{III} heterometallic centers bridged by dithiolato units of the TACN ligand, without metal–metal interaction (Ni1–Rh1 = 3.207(2) Å). The Ni1 atom retains a square-planar geometry as in **1a**; the interatomic distance of Ni1–N3 (2.614(7) Å) is appreciably shorter than that of **1a** (3.423(4) Å) with lone-pair electrons on the N3 atom directed to the Ni1 center. The Rh1 atom is ligated by η^5 -Cp* and a terminal Cl[−] ion. The structure of [3a]⁺ is essentially similar to that of [2a]⁺ (Ni1–Rh1 = 3.2128(6) Å, Ni1–N3 = 2.601(4) Å), except that the Cl[−] anion coordinating to Rh1 is replaced by a nitrate anion with a monodentate fashion.

By a method similar to that of $[2a]Cl$, reaction of $1b$ with 0.5 equiv of $[RhCp^*Cl_2]_2$ in a mixed solvent of chloroform/methanol was carried out, but any multinuclear complexes were not isolated in pure form. Alternatively, reaction of $^iPrTACN-S_2H_2$ with 1 equiv of $NiCl_2 \cdot 6H_2O$, followed by addition of 0.5 equiv of $[RhCp^*Cl_2]_2$ in one pot, afforded a dinuclear $NiRh$ complex $[2b]Cl$ that was purified by chromatography on an alumina column (Scheme 1). Complex $[2b]Cl$ has high solubility in H_2O (55 mg/mL at 20 °C) and is stable in water in a range of pH 2–11 confirmed by ESI-MS spectra. To the solution of $[2b]Cl$ in H_2O was added NH_4PF_6 to provide a red powder of $[2b]PF_6$. Treatment of $[2b]Cl$ with anion-exchange resin in water also afforded $[2b]NO_3$ in good yield. The 1H NMR spectra of complexes $[2b]X'$ ($X' = Cl, NO_3, PF_6$) in $CDCl_3$ show only broad resonances, owing to paramagnetism of the Ni^{II} metallo fragment of $1b$. The ESI mass spectra of $[2a]PF_6$ is shown in Figure S3 in the Supporting Information. An ORTEP diagram for the complex cation of $[2b]PF_6$ is shown in Figure 3. The structure consists of a

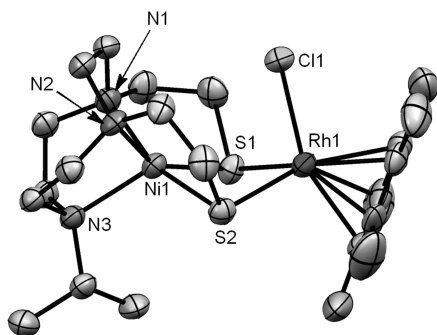
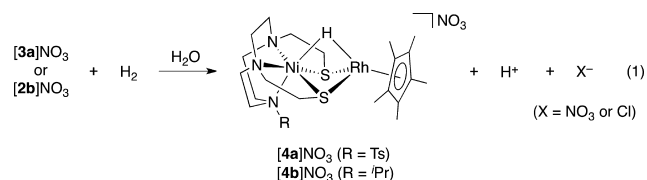


Figure 3. ORTEP drawing of $[2b]PF_6$. The counteranion (PF_6) and hydrogen atoms are omitted for clarity. Selected distances (Å) and angles (deg): $Ni1-Rh1 = 3.262(2)$, $Ni1-S1 = 2.323(2)$, $Ni1-S2 = 2.315(2)$, $Ni1-N1 = 2.097(6)$, $Ni1-N2 = 2.057(6)$, $Ni1-N3 = 2.101(6)$, $Rh1-S1 = 2.424(3)$, $Rh1-S2 = 2.400(3)$, $Rh1-Cl1 = 2.410(2)$, $Ni1-S1-Rh1 = 86.79(7)$, $Ni1-S2-Rh1 = 87.57(6)$.

$Ni^{II}Rh^{III}$ dinuclear core ($Ni1-Rh1 = 3.262(2)$ Å) essentially similar to that of $[2a]OTf$. Unlike complex $[2a]OTf$, the $Ni1$ atom adopts a distorted square-pyramidal geometry (τ value = 0.20),²⁰ where the $Ni1-N3$ length (2.101(6) Å) is significantly shorter than that of 2.614(7) Å in $[2a]OTf$ due to the strong σ -donating property of the $N3$ atom with an iPr group. These results clearly demonstrated that the steric and electronic structures of the Ni^{II} center of the dinuclear scaffold $[Ni(RTACN-S_2)RhCp^*Cl]^+$ can be varied depending on the substituent group on the $N3$ amino nitrogen.

Hydride-Bridged $Ni^{II}Rh^{III}$ Dinuclear Complexes $[(RTACN-S_2)Ni(\mu-H)RhCp^*]NO_3$ ($R = Ts$ ($[4a]NO_3$), iPr ($[4b]NO_3$)). Complex $[3a]NO_3$ readily reacted with H_2 (0.1 MPa) in H_2O (pH 7) at room temperature to give a hydride-bridged $Ni^{II}Rh^{III}$ complex $[(TsTACN-S_2)Ni(\mu-H)RhCp^*]NO_3$ ($[4a]NO_3$) in good yield (eq 1). The hydride complex



$[4a]NO_3$ was also synthesized from reaction of $[3a]NO_3$ with $HCOONa$ in H_2O at room temperature through β -hydrogen elimination with evolution of CO_2 . Complex $[2b]NO_3$ reacted with H_2 under a similar condition for $[3a]NO_3$ to afford $[(^iPrTACN-S_2)Ni(\mu-H)RhCp^*]NO_3$ ($[4b]NO_3$), but its isolated yield was very low. Kinetic analyses by monitoring the decrease of the absorption band at 305 nm for $[3a]NO_3$ and 254 nm for $[2b]NO_3$ revealed that the reactions with H_2 (0.1 MPa) at pH 7.0 at 20 °C proceeded with pseudo-first-order kinetics over four half-lives, as shown in Figures S11 and S12 (Supporting Information). The rate of the reaction of $[3a]NO_3$ with H_2 ($k_{obs} = 1.9 \times 10^{-2} s^{-1}$) is significantly faster than that of $[2b]NO_3$ ($k_{obs} = 4.5 \times 10^{-3} s^{-1}$) under the same conditions.

The ESI mass spectrum of $[4a]NO_3$ in MeOH (Figure S5a–c, Supporting Information) showed a prominent signal at m/z 697.99 with a characteristic distribution of isotopomers that matched well the calculated isotopic distribution for $[4a]^+$. To confirm the origin of the hydride, $[3a]NO_3$ was reacted with D_2 in H_2O (pH 7) for 5 h at room temperature, and the reaction product was analyzed by ESI-MS (Figure S5d–f, Supporting Information) to show that the signal at m/z 697.99 for $[4a]^+$ was shifted to 698.96, corresponding to $[(TsTACN-S_2)Ni(\mu-D)RhCp^*]^+$ ($[4a-d]^+$). Similarly, in the ESI mass spectrum of $[4b]NO_3$ in MeOH (Figure S6a–c, Supporting Information), the signal at m/z 585.98 was shifted to m/z 587.05 by using D_2 instead of H_2 (Figure S6d–f, Supporting Information). These mass spectral results clearly demonstrated that the hydride complexes $[4a]NO_3$ and $[4b]NO_3$ were generated through heterolytic cleavage of H_2 (eq 1). The IR spectrum of $[4a]NO_3$ (Figure S8, Supporting Information) exhibited a peak at 1923 cm^{-1} , which falls between the values for terminal (2250–1700 cm^{-1}) and bridging (1700–1200 cm^{-1}) metal–hydride units and might be assigned to the asymmetrical semibridging hydride of $\nu(Ni-H-Rh)$.²¹ The peak was definitely shifted to 1374 cm^{-1} in $[4a-d]NO_3$, and the energy difference (549 cm^{-1}) was consistent with replacement of the hydride H by the D atom. In the IR spectrum of $[4b]NO_3$ (Figure S9, Supporting Information), a peak at 1937 cm^{-1} was assigned to $\nu(Ni-H-Rh)$ and indicated that the semibridging character of the hydride ligand of $[4b]NO_3$ may be reduced in comparison with that in $[4a]NO_3$, presumably due to stronger *trans* influence of the amino group connected to the iPr substituent.

The detailed structure of $[4a]NO_3$ was determined by an X-ray analysis. The asymmetric unit involves two independent, chemically identical cations of $[4a]^+$ and two NO_3^- anions, together with three water molecules, and an ORTEP drawing for one of the cations is illustrated in Figure 4 (the diagram of the other cation is shown in Figure S10, Supporting Information). The complex contains $Ni^{II}Rh^{III}$ dimetal centers bridged by two thiolato units and a hydride ligand. The $\mu-H$ atom was determined by difference Fourier syntheses to reveal a semibridging mode mainly interacting with the Rh center. The Ni atom adopts a considerably distorted octahedral geometry with the N_3S_2 pentadentate ligand and the hydride anion. The $Ni-N3/N7$ distance for $[4a]NO_3$ (2.188(3), 2.192(3) Å), is fairly shorter than those for $[2a]OTf$ (2.614(7) Å) and $[3a]NO_3$ (2.601(4) Å). Furthermore, the dihedral angles defined by $Ni(\mu-S)_2$ and $Rh(\mu-S)_2$ for $[4a]NO_3$ (76.09°, 75.96°) are significantly smaller than those for $[2a]OTf$ (134.455°) and $[3a]NO_3$ (135.371°), and then the $Ni \cdots Rh$ distance for $[4a]NO_3$ (2.6921(6), 2.6906(6) Å) is concomitantly shorter than those for $[2a]OTf$ (3.207(2) Å)

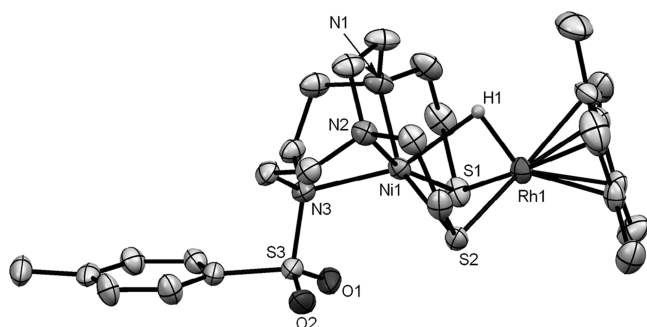


Figure 4. ORTEP drawing for one of the complex cations of $[4a]NO_3$. Selected distances (Å) and angles (deg): Ni1–Rh1 = 2.6921(6), Ni1–H1 = 2.18(5), Ni1–S1 = 2.3087(11), Ni1–S2 = 2.3312(12), Ni1–N1 = 2.068(4), Ni1–N2 = 2.057(4), Ni1–N3 = 2.188(3), Rh1–S1 = 2.3986(11), Rh1–S2 = 2.3856(10), Rh1–H1 = 1.66(5), Ni1–S1–Rh1 = 69.74(3), Ni1–S2–Rh1 = 69.59(4).

and $[3a]NO_3$ (3.2130(6) Å). These structural features of $[4a]NO_3$ demonstrated that the flexible dithiolato bridges allow such an interesting structural change triggered by incorporating a hydride ligand that is in concert with coordination of the NT's pendant amino group. A similar tendency has been observed in the Ni(μ -H)Ru complex $[Ni^{II}(H_2O)(\mu-RS)_2(\mu-H)Ru^{II}(\eta^6-C_6Me_6)]NO_3$ ((RSH)₂ = *N,N'*-dimethyl-*N,N'*-bis-(mercaptoethyl)-1,3-propanediamine).^{9d}

An ORTEP drawing of $[4b]NO_3$ is shown in Figure 5. Although the overall structure of the complex cation of

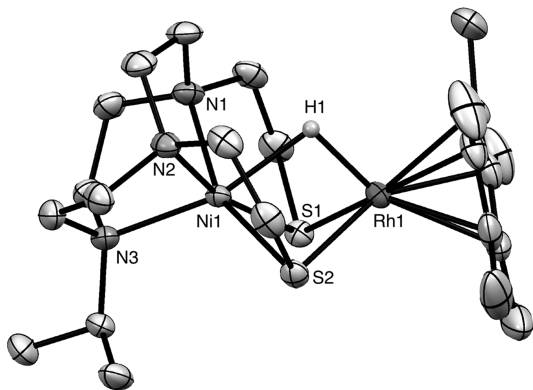


Figure 5. ORTEP drawing for the complex cation of $[4b]NO_3$. Selected distances (Å) and angles (deg): Ni1–Rh1 = 2.7228(4), Ni1–H1 = 2.03(5), Ni1–S1 = 2.3151(8), Ni1–S2 = 2.3395(8), Ni1–N1 = 2.069(2), Ni1–N2 = 2.107(2), Ni1–N3 = 2.056(2), Rh1–S1 = 2.3926(7), Rh1–S2 = 2.3568(7), Rh1–H1 = 1.50(4), Ni1–S1–Rh1 = 70.65(2), Ni1–S2–Rh1 = 70.87(2).

$[4b]NO_3$ is essentially identical to that of $[4a]NO_3$, the Ni–N3 bond length of $[4b]NO_3$ (2.056(2) Å) is notably shorter than the corresponding values of $[4a]NO_3$ (2.188(3), 2.192(3) Å), and the Ni···Rh interatomic distance (2.7228(4) Å) is appreciably elongated from those of $[4a]NO_3$ (av 2.6914 Å). These differences should result from the stronger σ -donating ability of the *N*ⁱPr amino group, which might cause a greater *trans* influence onto the bridging hydride. The less bridging character of the hydride in $[4b]NO_3$ is consistent with the IR spectrum. The ¹H NMR spectra of $[4a]NO_3$ and $[4b]NO_3$ showed only broad featureless signals, indicating that the complexes are paramagnetic, owing to the octahedral Ni^{II} center.

Stability of the isolated hydride complexes was examined. Both complexes $[4a]NO_3$ and $[4b]NO_3$ did not undergo an H/D exchange reaction under mild conditions in protic media. In particular, complex $[4a]NO_3$ was quite stable in water at pH 7–11 under N₂, and below ca. pH 6 (adjusted by the aqueous solution of HNO₃), complex $[4a]NO_3$ slowly decomposed to $[3a]NO_3$ with evolution of H₂. Formation of $[3a]NO_3$ was monitored by ESI-MS and UV–vis spectra. The first-order rate constant (*k*_{obs}) of the decomposition of $[4a]NO_3$ (under N₂, pH 4, 20 °C) was $2.7 \times 10^{-3} s^{-1}$ (Figure S13, Supporting Information). In contrast, the decomposition of $[4b]NO_3$ (under N₂, pH 4, 20 °C) was too fast to determine the rate constant accurately. These indicate that $[4a]NO_3$ is much more stable in H₂O than $[4b]NO_3$ because the hydride of $[4a]NO_3$ is assumed to be effectively stabilized by nesting between two metal centers.

Hydrogenation of Aldehydes Catalyzed by Dinuclear NiRh Complexes. Before we tried the hydrogenation of aldehydes into the corresponding alcohols catalyzed by the dinuclear NiRh complexes, some stoichiometric reactions were investigated. In the absence of H₂, benzaldehyde reacted with equimolar $[4a]NO_3$ in water (1 h, pH 7, 60 °C) to be reduced into benzyl alcohol in 8% yield. The low yield may be attributed to the instability of the hydride species in the reaction mixture. In contrast to $[4a]NO_3$, complex $[4b]NO_3$ did not reduce benzaldehyde at all under the same conditions because of the rapid decomposition of $[4b]NO_3$ in H₂O, which was confirmed by ESI-MS. Contrary to the air-sensitive hydride complexes, under catalytic conditions (H₂ = 0.1 MPa, pH 7, 60 °C), the air-stable precursor $[3a]NO_3$ has proven to catalyze the hydrogenation of benzaldehyde into benzyl alcohol in a yield of 92% after 12 h. As shown in Table 1, the catalytic activities for hydrogenation of benzaldehyde are dependent on the pH of the reaction solutions (entries 1–4). The initial TOFs (turnover frequencies after 1 h) of the hydrogenation of benzaldehyde showed a maximum at pH 7. This pH dependence might be related to both the stability of the hydride complex $[4a]NO_3$ and the activation process of

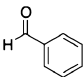
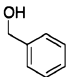
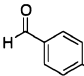
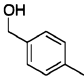
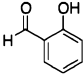
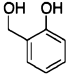
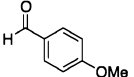
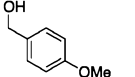
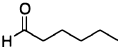
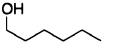
Table 1. Hydrogenation of Benzaldehyde in Aqueous Solutions Catalyzed by Dinuclear NiRh Complexes and Mononuclear Rh Complexes^a

entry	catalyst	pH	T (°C)	TOF ^b	TON ^c	yield (%) ^d
1	$[3a]NO_3$	3	60	2	16	32
2	$[3a]NO_3$	6	60	8	32	63
3	$[3a]NO_3$	7	60	22	46	92
4	$[3a]NO_3$	8	60	18	43	85
5	$[3a]NO_3$	7	20	0	2	4
6	$[3a]NO_3$	7	40	10	31	61
7	$[2b]NO_3$	7	60	0	2	4
8	$[2b]NO_3$	10	60	0	2	3
9	$[Cp^*Rh(bpy)Cl]Cl$	7	60	2	15	29
10	$Cp^*Rh(NO_3)_2$	7	60	6	21	51

^aBenzaldehyde was treated with H₂ in the presence of the catalyst in aqueous buffer solutions as described in the Experimental Section for 12 h. Conditions: catalyst = 5 μ mol (2.5 mM), substrate = 250 μ mol (125 mM), H₂ = 0.1 MPa, buffer solution = 2 mL. ^bTOF: initial turnover frequency ((mol of product)/(mol of catalyst))/h, determined by ¹H NMR analysis after 1 h. ^cTON: turnover number ((mol of product)/(mol of catalyst)), determined by ¹H NMR analysis after 12 h. ^dDetermined after 12 h.

aldehydes by protons.^{3j,5b,22} The rates of hydrogenation of benzaldehyde are also dependent on the temperature of the solutions (entries 3, 5, and 6), indicating that the higher the temperature, the faster the rate of the hydrogenation in the range of 20–60 °C. Complex **[2b]**NO₃ was almost inactive, and the mononuclear Rh complexes, such as [RhCp*Cl(bpy)]Cl and [RhCp*(NO₃)₂], showed only lower catalytic activities than that of **[3a]**NO₃, probably because the corresponding hydride species were unstable in H₂O or they did not activate H₂ in the conditions (entries 7–10). Hydrogenation of a variety of aldehydes was promoted by **[3a]**NO₃ at pH 7 at 60 °C (Table 2). Both aromatic (entries 1–4) and aliphatic

Table 2. Hydrogenation of Aldehydes in Aqueous Solutions Catalyzed by **[3a]NO₃^{a,b,c,d}**

Entry	Substrate	Product	TOF ^b	TON ^c	Yield (%) ^d
1			22	46	92
2			11	45	89
3			2	15	29
4			2	13	25
5			9	35	69

^aConditions: catalyst = 5 μmol (2.5 mM), substrate = 250 μmol (125 mM), H₂ = 0.1 MPa, T = 60 °C, buffer solution = 2 mL, pH 7. ^bTOF: initial turnover frequency ((mol of product)/(mol of catalyst)/h), determined by ¹H NMR analysis after 1 h. ^cTON: turnover number ((mol of product)/(mol of catalyst)), determined by ¹H NMR analysis after 12 h. ^dDetermined after 12 h.

aldehydes (entry 5) are converted to the corresponding alcohols. Hydrogenation of benzaldehyde (entry 1) proceeded much more efficiently than that of benzaldehyde derivatives with electron-donating groups, such as *p*-tolualdehyde, salicylaldehyde, and *p*-anisaldehyde (entries 2–4). The catalytic cycle in H₂O at pH 7 may involve formation of the hydride-bridged complex **[4a]**⁺ from heterolytic activation of H₂ by the Ni^{II}Rh^{III} species **[3a]**⁺ and reduction of the aldehydes by **[4a]**⁺ to restore the starting compound (Scheme 2).

Hydrogenation of CO₂ with Dinuclear NiRh Complexes. We have further investigated the hydrogenation of CO₂ into formate catalyzed by the dinuclear NiRh complexes.^{4a,d,23} The NiRh dinuclear complexes **[2a]**Cl, **[3a]**NO₃, and **[2b]**NO₃, together with the mononuclear Rh complexes, were examined under 2 MPa pressure of H₂ and CO₂ (1:1) in H₂O at 20 °C, and the product HCOO[−] was quantified by ¹H NMR (Table 3). Complex **[3a]**NO₃ effectively catalyzed the hydrogenation of CO₂ in H₂O under both acidic and basic conditions (entries 1–3). The catalytic activity of **[3a]**NO₃ (entry 3) was comparable to that of **[2a]**Cl (entry 4), suggesting that the hydride complex **[4a]**⁺ is an active species. Complex **[4a]**NO₃ was also a fair catalyst for the CO₂ hydrogenation with a lower TON by 33% than the

Scheme 2

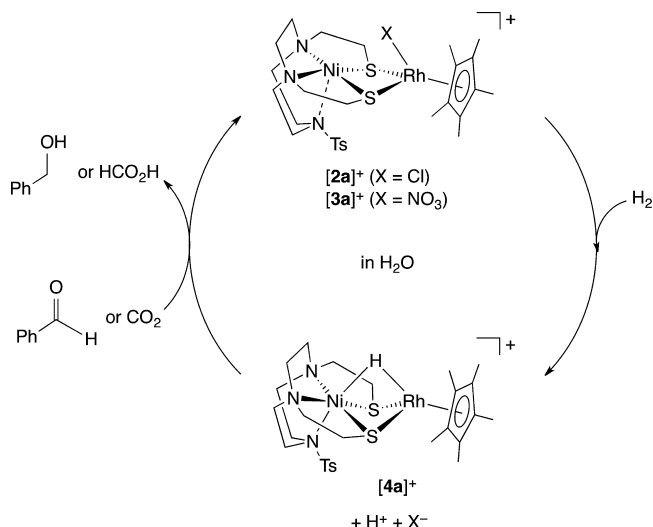


Table 3. Hydrogenation of CO₂ or Bicarbonate in Aqueous Solutions Catalyzed by Dinuclear NiRh Complexes and Mononuclear Rh Complexes^a

entry	catalyst	pH	TON ^b
1	[3a] NO ₃	4	10
2	[3a] NO ₃	7	16
3	[3a] NO ₃	11	34
4	[2a] Cl	11	38
5	[4a] NO ₃	11	23
6	[2b] NO ₃	4	0
7	[2b] NO ₃	7	0
8	[2b] NO ₃	11	1
9	[2b] Cl	11	1
10	[Cp*Rh(bpy)Cl]Cl	11	1
11	Cp*Rh(NO ₃) ₂	11	0

^aConditions: catalyst = 5 μmol (1 mM), H₂ = 1 MPa, CO₂ = 1 MPa, T = 20 °C, t = 20 h, buffer solution = 5 mL. ^bTON: turnover number ((mol of product)/(mol of catalyst)), determined by ¹H NMR analysis of the reaction mixture samples.

corresponding starting complex **[3a]**NO₃ (entry 5). Contrasted to the NiRh complexes with the TsTACN-S₂ ligand, complex **[2b]**NO₃ with the ⁱPrTACN-S₂ ligand (entries 6–8) and the mononuclear Rh complexes (entries 10 and 11) showed almost no activity. Although Himeda et al. have reported that [RhCp*Cl(bpy)]Cl catalyzed the hydrogenation of CO₂ in H₂O under higher temperature and pressure (80 °C, 4 MPa (CO₂/H₂ = 1:1)),^{23g} it showed only slight activity under the present conditions (20 °C, 2 MPa (CO₂/H₂ = 1:1)) because the postulated terminal hydride species [RhCp*(H)(bpy)]⁺ should be quite unstable in water. The catalytic cycle of hydrogenation of CO₂ with **[2a]**Cl or **[3a]**NO₃ was estimated as follows.^{4d,23h} The dinuclear NiRh complexes reacted with H₂ in H₂O to afford the hydride complex **[4a]**⁺, which may be much more stable in water than **[4b]**⁺ and the mononuclear species [RhCp*(H)(bpy)]⁺, and consequently, the hydride **[4a]**⁺ was able to react with CO₂ to afford formate. In the reaction solution of **[2a]**Cl with 2 MPa of H₂ and CO₂ (1:1), only **[2a]**⁺ and **[4a]**⁺ were observed by ESI-MS and no other NiRh dimetallic species was detected, implying that reaction of **[4a]**⁺ and CO₂ is the rate-determining step, and a reason for

the low activity of $[2b]^+$ could be attributable to the instability of the corresponding hydride $[4b]^+$ in water.

CONCLUSIONS

The hydride-bridged $Ni^{II}Rh^{III}$ complexes, $[(RTACN-S_2)Ni(\mu-H)RhCp^*X]^+$ ($R = Ts$ ($[4a]^+$), iPr ($[4b]^+$)), were successfully synthesized by utilizing the new N_3S_2 dithiolato ligands, through heterolytic activation of H_2 by $[Ni(RTACN-S_2)-RhCp^*X]^+$ ($R = Ts$, $X = NO_3$ ($[3a]^+$); $R = ^iPr$, $X = Cl$ ($[2b]^+$)). The stability of the hydride in $[4a]^+$ and $[4b]^+$ could be tuned by varying the R group of the TACN ligand through *trans* influence across the Ni^{II} center. In fact, complex $[4a]^+$ with an electron-withdrawing Ts group was quite stable and capable of reducing benzaldehyde in water. Contrastingly, complex $[4b]^+$ with an electron-donating iPr group, quickly decomposed in water. In light of these results, hydrogenation of aldehydes and CO_2 in water has been established by using $[3a]^+$ and $[2a]^+$ as precursors of an active species, $[4a]^+$, and is interestingly contrasted to the inactive precursor $[2b]^+$ with $R = ^iPr$. The present study could provide valuable insights into developing new catalysts for hydrogenation and hydrogen-transfer reactions in aqueous media.

ASSOCIATED CONTENT

Supporting Information

Tables, figures, and CIF files giving ORTEP diagrams of $[3a]NO_3$ and $[4a]NO_3$; ESI-MS of $[2a]OTf$, $[2b]PF_6$, $[3a]NO_3$, $[4a]NO_3$, and $[4b]NO_3$; IR spectra of $[3a]NO_3$, $[4a]NO_3$, $[4a-d]NO_3$, and $[4b]NO_3$; UV-vis spectral changes for reactions of $[3a]NO_3$ and $[2b]NO_3$ with H_2 , and decomposition of $[4a]NO_3$ in H_2O ; and crystallographic data (with CIF) for **1a**, **1b**, $[2a]OTf \cdot Et_2O$, $[2b]PF_6$, $[3a]NO_3$, $[4a]NO_3 \cdot 1.5H_2O$, and $[4b]NO_3 \cdot 1.5H_2O$. This material is available free of charge via the Internet at <http://pubs.acs.org>.

AUTHOR INFORMATION

Corresponding Author

*E-mail: kure@cc.nara-wu.ac.jp (B.K.), tanase@cc.nara-wu.ac.jp (T.T.). Tel: +81 742 20 3394. Fax: +81 742 20 3847.

Notes

The authors declare no competing financial interest.

ACKNOWLEDGMENTS

This work was supported by a Grant-in-Aid for Scientific Research and that on Priority Area 2107 (nos. 22108521, 24108727) from the Ministry of Education, Culture, Sports, Science and Technology, Japan, and by Nara Women's University Grants for Research Projects. B.K. thanks Profs. S. Ogo (Kyushu University) and S. Fukuzumi (Osaka University) for valuable discussions.

REFERENCES

(1) (a) Li, C.-J.; Chan, T.-H. *Comprehensive Organic Reactions in Aqueous Media*, 2nd ed.; John Wiley & Sons, Inc.: Hoboken, NY, 2007. (b) Cornils, B.; Herrmann, W. A., Eds. *Aqueous-Phase Organometallic Catalysis: Concepts and Applications*, 2nd ed.; Wiley-VCH: Weinheim, Germany, 2004. (c) Horváth, I. T.; Joó, F., Eds. *Aqueous Organometallic Chemistry and Catalysis*; Kluwer Academic Publishers: Dordrecht, The Netherlands, 1995. (d) Lindström, U. M. *Chem. Rev.* **2002**, 102, 2751. (e) Fish, R. H. *Coord. Chem. Rev.* **1999**, 185/186, 569. (f) Joó, F.; Kathó, Á. *J. Mol. Catal. A* **1997**, 116, 3. (g) Koelle, U. *Coord. Chem. Rev.* **1994**, 135/136, 623. (h) Herrmann, W. A.; Kohlpaintner, C. W. *Angew. Chem., Int. Ed. Engl.* **1993**, 32, 1524.

(2) (a) Ikariya, T. *Bull. Chem. Soc. Jpn.* **2011**, 84, 1. (b) Woodmansee, D. H.; Pfaltz, A. *Chem. Commun.* **2011**, 47, 7912. (c) Morris, R. H. *Chem. Soc. Rev.* **2009**, 38, 2282. (d) Ito, M.; Ikariya, T. *Chem. Commun.* **2007**, 5134. (e) Special issue on hydrogenation and transfer hydrogenation: Krische, M. J., Sun, Y., Eds.; *Acc. Chem. Res.* **2007**, 40, 1237–1419. (f) Ikariya, T.; Murata, K.; Noyori, R. *Org. Biomol. Chem.* **2006**, 4, 393. (g) Samec, J. S. M.; Backvall, J.-E.; Andersson, P. G.; Brandt, P. *Chem. Soc. Rev.* **2006**, 35, 237. (h) Gladiali, S.; Alberico, E. *Chem. Soc. Rev.* **2006**, 35, 226. (i) Clapham, S. E.; Hadzovic, A.; Morris, R. H. *Coord. Chem. Rev.* **2004**, 248, 2201. (j) Noyori, R.; Ohkuma, T. *Angew. Chem., Int. Ed.* **2001**, 40, 40. (k) Noyori, R.; Hashiguchi, S. *Acc. Chem. Res.* **1997**, 30, 97. (3) (a) Robertson, A.; Matsumoto, T.; Ogo, S. *Dalton Trans.* **2011**, 10304. (b) Delhomme, C.; Weuster-Botz, D.; Kühn, F. E. *Green Chem.* **2009**, 11, 13. (c) Wu, X.; Xiao, J. *Chem. Commun.* **2007**, 2449. (d) Joó, F. *Acc. Chem. Res.* **2002**, 35, 738. (e) Dwars, T.; Oehme, G. *Adv. Synth. Catal.* **2002**, 344, 239. (f) Sinou, D. *Adv. Synth. Catal.* **2002**, 344, 221. (g) Kure, B.; Matsumoto, T.; Ichikawa, K.; Fukuzumi, S.; Higuchi, Y.; Yagi, T.; Ogo, S. *Dalton Trans.* **2008**, 4747. (h) Papp, G.; Elek, J.; Nádasdi, L.; Laurenczy, G.; Joó, F. *Adv. Synth. Catal.* **2003**, 345, 172. (i) Süß-Fink, G.; Faure, M.; Ward, T. R. *Angew. Chem., Int. Ed.* **2002**, 41, 99. (j) Makihara, N.; Ogo, S.; Watanabe, Y. *Organometallics* **2001**, 20, 497. (k) Joó, F.; Kovács, J.; Bényei, A. Cs.; Kathó, Á. *Angew. Chem., Int. Ed.* **1998**, 37, 969. (4) (a) Tanaka, R.; Yamashita, M.; Nozaki, K. *J. Am. Chem. Soc.* **2009**, 131, 14168. (b) Frost, B. J.; Mebi, C. A. *Organometallics* **2004**, 23, 5317. (c) Vieille-Petit, L.; Therrien, B.; Süß-Fink, G.; Ward, T. R. *J. Organomet. Chem.* **2003**, 684, 117. (d) Hayashi, H.; Ogo, S.; Abura, T.; Fukuzumi, S. *J. Am. Chem. Soc.* **2003**, 125, 14266. (e) Faure, M.; Vallina, T.; Stoeckli-Evans, H.; Süß-Fink, G. *J. Organomet. Chem.* **2001**, 621, 103. (5) (a) Mebi, C. A.; Nair, R. P.; Frost, B. J. *Organometallics* **2007**, 26, 429. (b) Abura, T.; Ogo, S.; Watanabe, Y.; Fukuzumi, S. *J. Am. Chem. Soc.* **2003**, 125, 4149. (c) Kuo, L. Y.; Weakley, T. J. R.; Awana, K.; Hsia, C. *Organometallics* **2001**, 20, 4969. (d) Ogo, S.; Makihara, N.; Kaneko, Y.; Watanabe, Y. *Organometallics* **2001**, 20, 4903. (6) (a) Steckhan, E.; Herrmann, S.; Ruppert, R.; Dietz, E.; Frede, M.; Spika, E. *Organometallics* **1991**, 10, 1568. (b) Lo, H. C.; Buriez, O.; Kerr, J. B.; Fish, R. H. *Angew. Chem., Int. Ed.* **1999**, 38, 1429. (c) Lo, H. C.; Leiva, C.; Buriez, O.; Kerr, J. B.; Olmstead, M. M.; Fish, R. H. *Inorg. Chem.* **2001**, 40, 6705. (d) Canivet, J.; Süß-Fink, G.; Štěpnička, P. *Eur. J. Inorg. Chem.* **2007**, 4736. (7) (a) Special issue on hydrogenases: Darensbourg, M. Y., Weigand, W., Eds.; *Eur. J. Inorg. Chem.* **2011**, 915–1171. (b) Tard, C.; Pickett, C. J. *Chem. Rev.* **2009**, 109, 2245. (c) Fontecilla-Camps, J. C.; Volbeda, A.; Cavazza, C.; Nicolet, Y. *Chem. Rev.* **2007**, 107, 4273. (d) Special issue on hydrogenases: Pickett, C.; Best, S., Eds.; *Coord. Chem. Rev.* **2005**, 249, 1517–1690. (e) Cammack, R.; Frey, M.; Robson, R. *Hydrogen as a Fuel: Learning from Nature*; Taylor & Francis: London, 2001. (f) Frey, M. *Structure and Bonding*; Springer-Verlag: Berlin, 1998; pp 97–126. (g) Albracht, S. P. J. *Biochim. Biophys. Acta* **1994**, 1188, 167. (8) (a) Vobeda, A.; Charon, M. H.; Piras, C.; Hatchikian, E. C.; Frey, M.; Fontecilla-Camps, J. C. *Nature* **1995**, 373, 580. (b) Volbeda, A.; Garcin, E.; Piras, C.; De Lacy, A. L.; Hatchikian, E. C.; Frey, M.; Fontecilla-Camps, J. C. *J. Am. Chem. Soc.* **1996**, 118, 12989. (c) Pandelia, M.-E.; Ogata, H.; Lubitz, W. *ChemPhysChem* **2010**, 11, 1127. (d) Ogata, H.; Lubitz, W.; Higuchi, Y. *Dalton Trans.* **2009**, 7577. (e) Lubitz, W.; Reijerse, E.; van Gestel, M. *Chem. Rev.* **2007**, 107, 4331. (9) (a) Ohki, Y.; Tatsumi, K. *Eur. J. Inorg. Chem.* **2011**, 973. (b) Canaguier, S.; Artero, V.; Fontecave, M. *Dalton Trans.* **2008**, 315. (c) Barton, B. E.; Whaley, C. M.; Rauchfuss, T. B.; Gray, D. L. *J. Am. Chem. Soc.* **2009**, 131, 6942. (d) Ogo, S.; Kabe, R.; Uehara, K.; Kure, B.; Nishimura, T.; Menon, S. C.; Harada, R.; Fukuzumi, S.; Higuchi, Y.; Ohhara, T.; Tamada, T.; Kuroki, R. *Science* **2007**, 316, 585. (10) The crystal structure of the protonated complex, $[Ni^{II}(OH_2)(\mu-SR)_2(\mu-H)Ru^{II}(\eta^6-C_6Me_6)](NO_3)$, was reported;^{9d} however, the complex did not show activity for the hydrogenations.^{3g}

- (11) (a) Halfen, J. A.; Tolman, W. B. *Inorg. Synth.* **1998**, 32, 75. (b) Sessler, J. L.; Sibert, J. W.; Lynch, V. *Inorg. Chem.* **1990**, 29, 4143. (c) Halfen, J. A.; Jazdzewski, B. A.; Mahapatra, S.; Berreau, L. M.; Wilkinson, E. C.; Que, L., Jr.; Tolman, W. B. *J. Am. Chem. Soc.* **1997**, 119, 8217. (d) Kang, J. W.; Moseley, K.; Maitlis, P. M. *J. Am. Chem. Soc.* **1969**, 91, 5970. (e) Hursthouse, M. B.; Malik, K. M. A.; Mingos, D. M. P.; Willoughby, S. D. *J. Organomet. Chem.* **1980**, 192, 235.
- (12) (a) Glasoe, P. K.; Long, F. A. *J. Phys. Chem.* **1960**, 64, 188. (b) Mikkelsen, K.; Nielsen, S. O. *J. Phys. Chem.* **1960**, 64, 632.
- (13) *Crystal Clear: Operating Software for the CCD Detector System*, version 1.3.5; Rigaku and Molecular Structure Corp.: Tokyo, Japan and The Woodlands, TX, 2003.
- (14) Jacobson, R. *REQAB*; Molecular Structure Corporation: The Woodlands, TX, 1998.
- (15) Sheldrick, G. M. *SHELXS-97 and SHELXL-97: Program for the Solution and the Refinement of Crystal Structures*; University of Göttingen: Göttingen, Germany, 1996.
- (16) (a) Altomare, A.; Burla, M. C.; Camalli, M.; Cascarano, M.; Giacovazzo, C.; Guagliardi, A.; Polidori, G. *J. Appl. Crystallogr.* **1994**, 27, 435–436. (b) Altomare, A.; Burla, M.; Camalli, M.; Cascarano, G.; Giacovazzo, C.; Guagliardi, A.; Moliterni, A.; Polidori, G.; Spagna, R. *J. Appl. Crystallogr.* **1999**, 32, 115–119.
- (17) *CrystalStructure 4.0: Crystal Structure Analysis Package*; Rigaku Corporation: Tokyo, Japan, 2000–2010.
- (18) (a) Houser, R. P.; Halfen, J. A.; Young, V. G., Jr.; Blackburn, N. J.; Tolman, W. B. *J. Am. Chem. Soc.* **1995**, 117, 10745. (b) Li, M.; Bonnet, D.; Bill, E.; Neese, F.; Weyhermüller, T.; Blum, N.; Sellmann, D.; Wieghardt, K. *Inorg. Chem.* **2002**, 41, 3444. (c) Moore, D. A.; Fanwick, P. E.; Welch, M. J. *Inorg. Chem.* **1990**, 29, 672.
- (19) (a) Stibrany, R. T.; Fox, S.; Bharadwaj, P. K.; Schugar, H. J.; Potenza, J. A. *Inorg. Chem.* **2005**, 44, 8234. (b) Rao, P. V.; Bhaduri, S.; Jiang, J.; Holm, R. H. *Inorg. Chem.* **2004**, 43, 5833. (c) Golden, M. L.; Yarbrough, J. C.; Reibenspies, J. H.; Darensbourg, M. Y. *Inorg. Chem.* **2004**, 43, 4702. (d) Grapperhaus, C. A.; Mullins, C. S.; Kozłowski, P. M.; Mashuta, M. S. *Inorg. Chem.* **2004**, 43, 2859. (e) Smeets, J. J.; Miller, M. L.; Grapperhaus, C. A.; Reibenspies, J. H.; Darensbourg, M. Y. *Inorg. Chem.* **2001**, 40, 3601. (f) Baidya, N.; Ndreu, D.; Olmstead, M. M.; Mascharak, P. K. *Inorg. Chem.* **1991**, 30, 2448. (g) Colpas, G. J.; Kumar, M.; Day, R. O.; Maroney, M. J. *Inorg. Chem.* **1990**, 29, 4779. (h) Mills, D. K.; Reibenspies, J. H.; Darensbourg, M. Y. *Inorg. Chem.* **1990**, 29, 4366. (i) Fernando, Q.; Wheatley, P. J. *Inorg. Chem.* **1965**, 4, 1726.
- (20) Addison, A. W.; Rao, T. N. *J. Chem. Soc., Dalton Trans.* **1984**, 1349.
- (21) Nakamoto, K. *Infrared and Raman Spectra of Inorganic and Coordination Compounds*, 6th ed.; John Wiley & Sons, Inc.: Hoboken, NJ, 2009.
- (22) Ogo, S.; Abura, T.; Watanabe, Y. *Organometallics* **2002**, 21, 2964.
- (23) (a) Wang, W.; Wang, S.; Ma, X.; Gong, J. *Chem. Soc. Rev.* **2011**, 40, 3703. (b) Himeda, Y. *Eur. J. Inorg. Chem.* **2007**, 3927. (c) Jessop, P. G.; Joo, F.; Tai, C.-C. *Coord. Chem. Rev.* **2004**, 248, 2425. (d) Jessop, P. G.; Ikariya, T.; Noyori, R. *Chem. Rev.* **1995**, 95, 259. (e) Federsel, C.; Jackstell, R.; Beller, M. *Angew. Chem., Int. Ed.* **2010**, 49, 6254. (f) Sanz, S.; Benítez, M.; Peris, E. *Organometallics* **2010**, 29, 275. (g) Himeda, Y.; Onozawa-Komatsuzaki, N.; Sugihara, H.; Kasuga, K. *Organometallics* **2007**, 26, 702. (h) Ogo, S.; Kabe, R.; Hayashi, H.; Harada, R.; Fukuzumi, S. *Dalton Trans.* **2006**, 4657.